THEMIS Observations of Long-lived Regions of Large-Amplitude Whistler Waves in the Inner Magnetosphere

C. M. Cully

Laboratory for Atmospheric and Space Physics, University of Colorado, Boulder, Colorado, USA.
Now at Swedish Institute of Space Physics, Uppsala, Sweden.

J. W. Bonnell

Space Sciences Laboratory, University of California, Berkeley, California, USA.

R. E. Ergun

Laboratory for Atmospheric and Space Physics, University of Colorado, Boulder, Colorado, USA.

Recent reports of large-amplitude whistler waves (>100 mV/m) in the radiation belts have intensified interest in the role of whistler waves in accelerating radiation belt electrons to MeV energies. Several critical parameters for addressing this issue have previously not been observed, including the occurrence frequency, spatial extent and longevity of regions of large-amplitude whistlers. The THEMIS mission, with multiple satellites in a near-equatorial orbit, offers an excellent opportunity to study these waves. We use data from the Electric Field Instrument (EFI) to show that the probability distribution of wave activity in the dawn radiation belts has a significant high-amplitude tail, and is hence not well-described by long-term time averages. Regions of enhanced wave activity exist with four-second averaged wave power above 1 mV/m and sub-second bursts up to several hundred mV/m. These regions are spatially localized to at most several hours of local time azimuthally, but can persist in the same location for several days. With large regions of space persistently covered by bursty, large-amplitude waves, the actual mechanisms and rates of radiation belt electron acceleration may need to be reconsidered.

Physical processes working in the outer Van Allen radiation belts can both accelerate particles to MeV energies and also rapidly drain the resulting energetic populations. Several acceleration mechanisms are known, including impulsive changes in the large-scale magnetic field configuration [*Li et al.*, 2001], drift-resonant interaction with Ultra-Low Frequency (ULF) waves [*Elkington et al.*, 2003; *Mann et al.*, 2004] and Doppler-shifted cyclotron-resonant interactions with whistler-mode waves [*Horne and Thorne*, 2003; *Meredith et al.*, 2003]. Since all of these acceleration mechanisms tend to be active simultaneously with a still-longer list of depletion mechanisms, the response of the system to its solar wind drivers is non-trivial [*Onsager et al.*, 2007].

Recent observations by *Cattell et al.* [2008] have shown the existence of whistler-mode waves with amplitudes in excess of 100 mV/m. The existence of these waves suggests a new paradigm for acceleration by whistler waves. Rather than being gradually energized by repeated interactions with weak whistlers (on the order 0.1 mV/m), radiation belt electrons may be abruptly accelerated by relatively few interactions with extremely intense waves. Simulations of electrons interacting with order 100 mV/m whistler waves show acceleration to MeV energies in as little as 0.1 s [*Cattell et al.*, 2008]. In order to quantitatively assess the role these waves play in radiation belt dynamics, several observational issues need to be addressed, including the occurrence frequency and amplitude distribution of the waves, and the spatial and temporal extent of the regions in which they are found.

The THEMIS mission [*Angelopoulos*, 2008] consists of 5 satellites in near-equatorial orbits with apogees above 10 Earth radii (R_E) and perigees below 2 R_E. Equipped with high-quality fields instruments, these satellites offer an excellent opportunity to study the characteristics of large-amplitude whistler waves in relevant regions of space.

In this paper, we present the first observations of large-amplitude whistler waves from the THEMIS Electric Fields Instrument (EFI). In section 1, we present a statistical analysis of the whistler amplitudes based on four-second averaged data. However, the highest amplitudes tend to have durations much less than four seconds, and hence are underrepresented in these statistics. In section 2, we present a burst of whistler activity of ~300 mV/m lasting for tenths of a second. Finally, we discuss the spatial and temporal extent of regions of large-amplitude whistler waves in section 3.

1. Wave Power Statistics

The Digital Fields Board (DFB) [*Cully et al.*, 2008] calculates the mean amplitude of the electric and magnetic fields in 6 logarithmically-spaced passbands up to 4 kHz using electric field data from the double-probe Electric Fields Instrument (EFI) [*Bonnell et al.*, 2008] and magnetic field data from the Search Coil Magnetometer (SCM) [*Roux et al.*, 2008]. The resulting amplitude values (filter bank data) are included in the survey mode telemetry, covering most orbits with a measurement cadence of four seconds. The EFI booms on probes C, D and E were deployed in the early summer of 2007; with near-continual coverage on three probes in near-equatorial orbits, the filter bank data from these instruments provide a solid foundation for a statistical analysis of wave power. The booms on the two remaining probes have now been successfully deployed, and we expect 5-probe coverage for 2008.

Between June and December 2007, there are a combined 73 million electric field filter bank spectra from probes C, D and E after removing bad data intervals (telemetry errors, intervals when the EFI was operating in diagnostic or non-optimal modes, spacecraft thruster firings, etc.). The leftmost panels of Figure 1 show the mean value of these data as binned by location in the xy plane in Geocentric Solar Magnetic (GSM) coordinates. The top left panel displays

0094-8276/08/$5.00

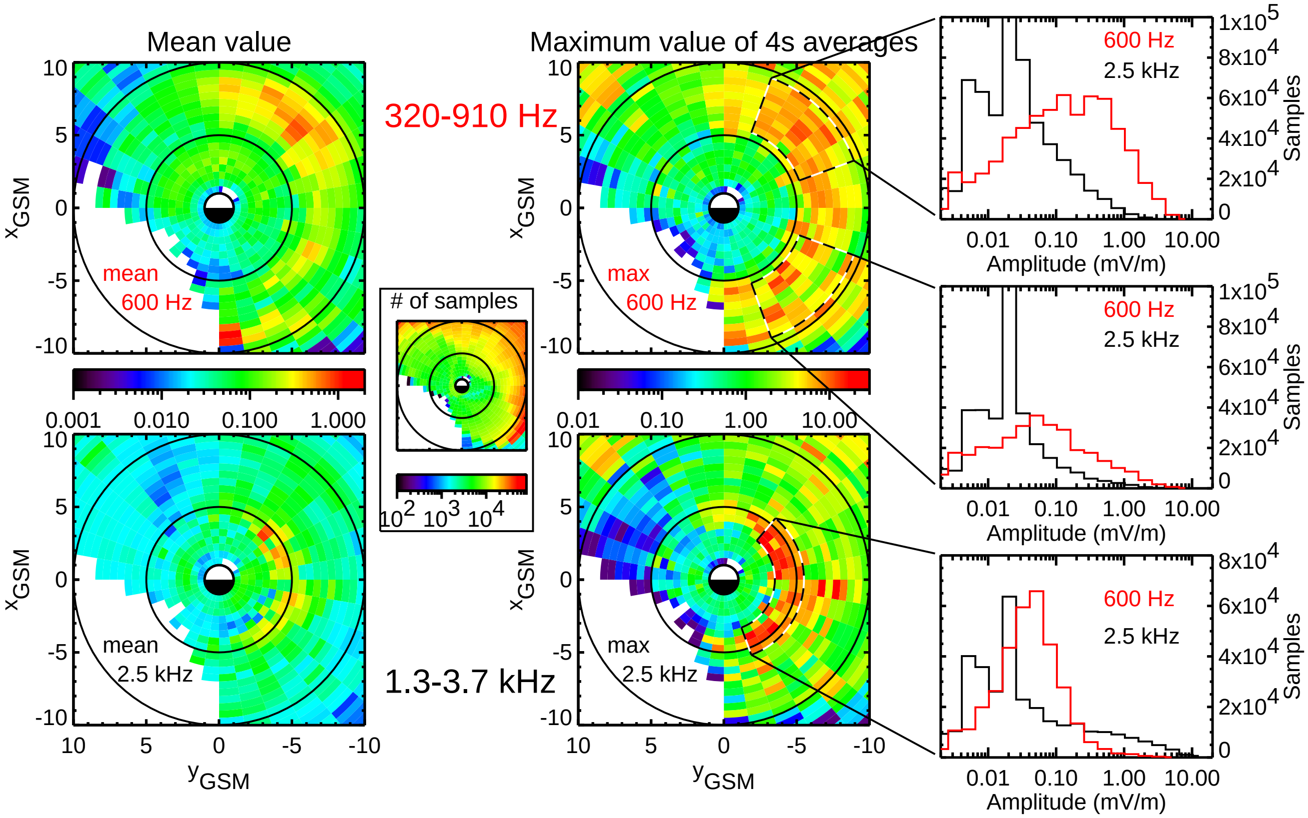

Figure 1. Wave amplitudes in mV/m from the filter bank data on THEMIS C,D and E. Left column: mean amplitude as a function of position in the GSM plane in the 600 Hz band (top) and 2.5 kHz band (bottom). Inset: number of filter bank spectra used in each cell in the left and middle columns. Middle column: maximum value of the four-second averaged filter bank data. Right column: histograms of the filter bank values in the regions shown.

mean power in the 600 Hz band (320 to 910 Hz), while mean power in the 2.5 kHz band (1.3 kHz to 3.7 kHz) is shown at the bottom left.

The upper whistler band, from 0.5 to 1.0 times the electron cyclotron frequency, overlaps with the 2.5 kHz band near 5 R_E, and with the 600 Hz band near 8 R_E. Localized intensity peaks exist at these distances on the dawn side in the corresponding frequency band (Figure 1). The mean amplitudes reach 1 to 2 mV/m in these enhanced regions, consistent with the results of *Meredith et al.* [2001] based on CRRES data.

Although the mean value has interest in and of itself, the radiation belt particles may be energized by relatively rare large-amplitude events, rather than frequent low-amplitude events. To investigate such large-amplitude waves, we first plot the maximum value of the (four-second averaged) filter bank data as a function of position in the middle panels of Figure 1. The dawn sector again exhibits large amplitudes, with peak intensities of 30 mV/m in the 2.5 kHz band near 5 R_E, and peak intensities near 8-10 mV/m in the 600 Hz band near 8 R_E. We stress that these "maximum values" have still been averaged over four seconds; instantaneous amplitudes can greatly exceed these four-second averages, as will be shown in section 2.

The geophysical role of these large-amplitude waves depends on the probability distribution of the wave amplitude, which is shown in the histograms in the rightmost panels of Figure 1. Data for these three histograms has been selected from the three regions shown. The probability distribution for 2.5 kHz in the dawn sector near 5 R_E (bottom panel, black) is particularly interesting; although the distribution is exponentially bounded (and hence not heavy-tailed in the formal sense), a substantial fraction of the total probability is contained in the tail of the distribution. The median and mean values for the wave amplitude in this region are only 0.03 and 0.4 mV/m respectively, while the probability of observing waves with four-second averaged amplitudes larger than 4 mV/m (i.e. an order of magnitude greater than the mean) is 2.5%.

During most of 2007, the filter banks used AC-coupled data from the EFI instrument with a measurement range of ± 80 mV/m at 1 kHz. Consequently, the largest-amplitude waves saturate the data stream used by the filter banks. This effect will tend to truncate the tail of the distribution and reduce the maximum values (middle panels of Figure 1). For the 2008 season, we may use DC-coupled data with a saturation threshold of 500 mV/m.

2. High-resolution waveforms

The EFI also captures waveform data at rates up to 16 kS/s during short burst intervals, some of which were scheduled to coincide with the radiation belt encounters. The burst data give brief snapshots of the waveforms that are averaged into the filter bank data in section 1.

In regions of low-amplitude waves, the wave power may be relatively steady over the four-second interval, in which case the filter bank value gives a good representation of the wave amplitude. However, in regions of high-amplitude waves, the burst waveforms present a very different picture. Instead of relatively constant wave amplitudes, the amplitude fluctuates dramatically over several orders of magnitude. Such intermittent, bursty signals are not well represented by the four-second averaged filter bank data.

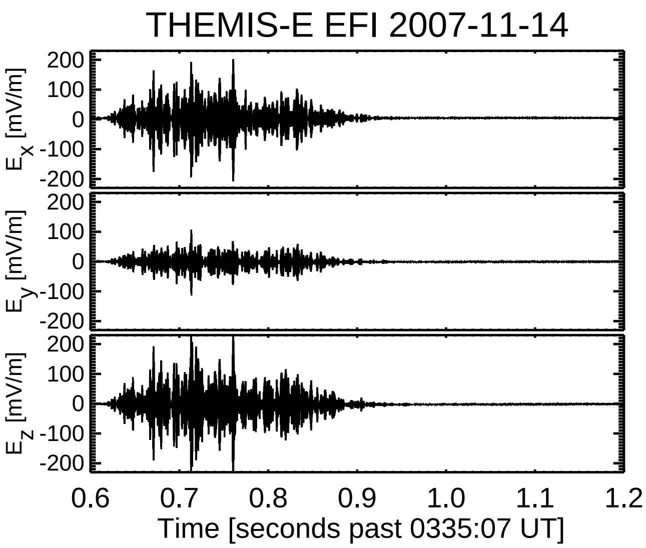

Figure 2. Three component EFI electric field data in GSM coordinates. Sampling rate is 8192 Hz.

The burst of wave power in Figure 2 was captured by THEMIS E at a radial distance of 4.0 R_E, and is a particularly extreme example of an intense burst embedded in an otherwise relatively quiet environment. The burst lasts for about 0.3 seconds, with a peak amplitude reaching over 300 mV/m. The burst is extremely isolated; the filter banks report a four-second averaged amplitude of only 0.4 mV/m. However, the longer interval surrounding this burst shows enhanced wave activity, with filter bank values in the 10 minutes before and after varying over a wide range from 0.05 to 5 mV/m.

The data in figure 2 has been corrected by both deconvolving the instrument response and correcting for the effective boom lengths. However, the waves were near the Nyquist frequency for the 8192 Hz sampling rate; some of the signal is therefore aliased from higher frequencies, and the signal amplitude therefore underestimated. Based on the (1 kHz) bandwidth of the observed (aliased) signal, the power at 4-6 kHz in the onboard power spectra and the analog filter characteristics, the amplitude is underestimated by at most a factor of 40%, and more likely 10 to 20%.

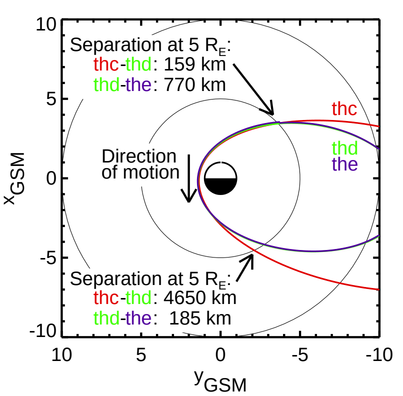

Figure 3. Orbits for THEMIS C, D and E on 16 November 2007. The orbits for THEMIS D and E are extremely similar, and are difficult to distinguish.

3. Spatial and Temporal Extent of Large-Amplitude Waves: A Case Study

In November and December 2007, the THEMIS constellation underwent re-positioning maneuvers to transition from from the coast orbits to the final orbits. On 16 November 2007, THEMIS D and E had nearly identical trajectories, (Figure 3), with D leading by about 1 hour and 40 minutes. Probe C had a higher apogee and a longer period, but all three probes cut through 5 R_E at similar local times. On the inbound leg of the orbit, all three probes passed through nearly the same location at 5 R_E, while THEMIS C intersected the 5 R_E circle about 4600 km ($\sim$0.5 hours local time) from the other 2 probes on the outbound leg. The inbound and outbound legs on probes D and E were separated by 6.7 hours in local time.

Between 13 and 18 November 2007, the THEMIS satellites encountered regions of enhanced whistler wave power (filter bank values greater than 1 mV/m) on multiple passes. Wave power in the 2.5 kHz band was minimal on 12 November, but starting on 13 November, wave power began to build on the outbound legs. Wave power on the outbound leg remained high during passes on 13-14 November, and then diminished on 15 November (Figure 4, panel a). Starting on 16 November, wave power then began to build on the inbound leg (panels b-f), reaching high and sustained values through 17 November before returning to low values on 18 November (panel g).

In total, 85 brief burst-mode waveforms were captured in the radiation belts during the interval between 13-17 November 2007. Although the largest observed amplitudes occur

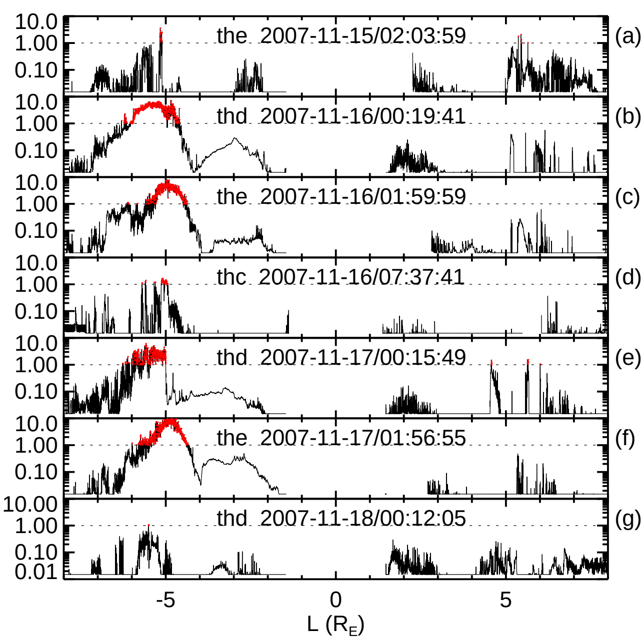

Figure 4. Filter bank amplitude in the 2.5 kHz band as a function of magnetic equatorial radius L. The inbound leg of each orbit has been assigned L<0 to distinguish it from the outbound leg. Panels are arranged chronologically. Values below 0.015 mV/m have been plotted at 0.015 mV/m to distinguish low amplitudes from data gaps.

in the burst data shown in section 2, large-amplitude waves (many tens to hundreds of mV/m) appear repeatedly in the other bursts when nearby filter bank values are larger than about 1 mV/m. In association with the filter bank data in Figure 4, showing a persistent region of enhanced wave power, we conclude that regions of large-amplitude whistlers can persist in a similar location for days.

By comparing the various passes in Figure 3, we can roughly estimate the size of the region of enhanced whistler power. First, enhanced power (>1 mV/m) is seen on the inbound leg (13-14 November, not shown) or on the outbound leg (panels b,c,e,f) but not both. Thus, the waves are azimuthally localized to at most 6 hours of local time, and do not cover the whole dawn sector simultaneously. Also, although probes D and E observed similar large amplitudes on both 16 and 17 November (panels b,c,e,f), probe C saw substantially smaller signals (panel d). Since the outbound leg of probe C was separated from those of D and E by only 0.5 hours local time, we conclude that the regions of large-amplitude waves have well-defined edges. Since it seems unlikely that THEMIS D and E would encounter the region so repeatably if it were extremely small, we conclude that the region of intense emissions is localized, with an azimuthal extent between 1 and 4 hours in local time. The radial extent ($\sim$1 R_E) is dictated by the measurement frequency band (1.3 to 3.7 kHz) and has little geophysical meaning; at larger distances, the electron cyclotron frequency is lower, so that the upper whistler band no longer falls in the range of the bandpass filter.

Advanced Composition Explorer (ACE) data for the relevant dates show an interval of high speed solar wind (600 km/s) starting on 13 November 2007. Geomagnetic activity was low to moderate, likely due to a fluctuating z component of the interplanetary magnetic field. The THEMIS ground-based magnetometer array observed a number of substorms and smaller disturbances, but no major events. The provisional AE index was quiet to moderate, and the Kp index remained at or below 3+. The provisional DST index was quiet, with no excursions below -30 nT over the interval in Figure 4. These conditions (high-speed solar wind, low to moderate geophysical activity) are associated with effective radiation belt particle acceleration [*O'Brien et al.*, 2001; *Onsager et al.*, 2007] and increased whistler-mode chorus emissions [*Hwang et al.*, 2007].

4. Conclusions

The THEMIS filter bank data are used to paint a broad picture of the wave activity in the inner magnetosphere. Using the four-second averaged data, the average amplitude of whistler waves in the dawn chorus region is several mV/m, consistent with previous results [*Meredith et al.*, 2001]. However, the probability distribution of the wave amplitudes has significant probability far out into the tail, which makes average values potentially misleading. The distribution of several kHz power in the dawn sector near 5 R_E has a particularly "heavy" tail, with 2.5% of the samples having an amplitude greater then an order of magnitude larger than the mean.

Burst data show that there are still greater wave amplitudes than those seen in the four-second averaged filter bank data. Waves with amplitudes >100 mV/m are observed, and are usually confined to short-duration packets which tend not to show up in four-second averages.

Large-amplitude waves are observed in a localized region with a long lifetime. The case study presented time-averaged wave amplitudes in the 2.5 kHz band of roughly 10 mV/m, with bursts to several hundred mV/m. The region of enhanced activity persisted for several days, and was localized azimuthally, with an extent of several hours. The region wandered in azimuth over several days, appearing first near 02 local time, and then later near 09 local time.

Whistler waves with amplitude >100 mV/m can dramatically accelerate electrons in their vicinity; *Cattell et al.* [2008] predicted acceleration to MeV energies in less than 0.1 s. Much of the previous work on the mechanisms and rates of relativistic electron acceleration via dawn chorus [e.g. *Horne et al.*, 2005, and references therein] has used time-averaged spectral densities which may not be fully representative of the true conditions, as discussed above. With large regions of space covered by bursty, large-amplitude waves, the actual mechanisms and rates may be qualitatively or quantitatively different.

In addition to acceleration, whistler waves can also scatter electrons into the loss cone, which results in a net loss of energetic particles. Their role in depletion of the energetic electron population is a similarly open question. We anticipate that future studies will quantify the effect of these whistler waves on both the acceleration and depletion of energetic radiation belt particles.

Acknowledgments. This research was funded by NASA contract NAS5-02099 (THEMIS). The THEMIS project has been made possible by many individuals whom we thank greatly, including V. Angelopoulos and F. Mozer whom we acknowledge for use of EFI data. We acknowledge the WDC for Geomagnetism, Kyoto University, Japan for the geomagnetic indices, and D. J. McComas, N. Ness and CDAWeb for the ACE data.

References

Angelopoulos, V. (2008), The THEMIS mission, *Space Sci. Rev.*, submitted.

Bonnell, J., et al. (2008), The electric field experiment on the THEMIS satellites, *Space Sci. Rev.*, submitted.

Cattell, C., et al. (2008), Discovery of very large amplitude whistler-mode waves in earth's radiation belts, *Geophys. Res. Lett.*, *35*(L01105), doi:10.1029/2007GL032009.

Cully, C. M., R. E. Ergun, K. Stevens, A. Nammari, and J. Westfall (2008), The THEMIS Digital Fields Board, *Space Sci. Rev.*, submitted.

Elkington, S. R., M. K. Hudson, and A. A. Chan (2003), Resonant acceleration and diffusion of outer zone electrons in an asymmetric geomagnetic field, *J. Geophys. Res.*, *108*(A3), doi: 10.1029/2001JA009202.

Horne, R. B., and R. M. Thorne (2003), Relativistic electron acceleration and precipitation during resonant interactions with whistler-mode chorus, *Geophys. Res. Lett.*, *30*(10), doi: 10.1029/2003GL016973.

Horne, R. B., R. M. Thorne, S. A. Glauert, J. M. Albert, N. P. Meredith, and R. R. Anderson (2005), Timescale for radiation belt electron acceleration by whistler mode chorus waves, *J. Geophys. Res.*, *110*(A03225), doi:10.1029/2004JA010811.

Hwang, J. A., D.-Y. Lee, L. R. Lyons, A. J. Smith, S. Zou, K. W. Min, K.-H. Kim, Y.-J. Moon, and Y. D. Park (2007), Statistical significance of association between whistler-mode chorus enhancements and enhanced convection periods during high-speed streams, *J. Geophys. Res.*, *112*(A09213), doi: 10.1029/2007JA012388.

Li, X., M. Temerin, D. N. Baker, G. D. Reeves, and D. Larson (2001), Quantitative prediction of radiation belt electrons at geostationary orbit based on solar wind measurements, *Geophys. Res. Lett.*, *28*(9), 1887–1890.

Mann, I. R., T. P. O'Brien, and D. K. Milling (2004), Correlations between ULF wave power, solar wind speed, and relativistic electron flux in the magnetosphere: solar cycle dependence, *J. Atmos. Sol. Terr. Phys.*, *66*, 187–198.

Meredith, N. P., R. B. Horne, and R. R. Anderson (2001), Substorm dependence of chorus amplitudes: Implications for the acceleration of electrons to relativistic energies, *J. Geophys. Res.*, *106*(A7), 13,165–13,178.

Meredith, N. P., M. Cain, R. B. Horne, R. M. Thorne, D. Summers, and R. R. Anderson (2003), Evidence for chorus-driven electron acceleration to relativistic energies from a survey of geomagnetically disturbed periods, *J. Geophys. Res.*, *108*(A6), doi:10.1029/2002JA009764.

O'Brien, T. P., R. L. McPherron, D. Sornette, G. D. Reeves, R. Friedel, and H. J. Singer (2001), Which magnetic storms produce relativistic electrons at geosynchronous orbit?, *J. Geophys. Res.*, *106*(A8), 15,533–44.

Onsager, T. G., J. C. Green, G. D. Reeves, and H. J. Singer (2007), Solar wind and magnetospheric conditions leading to the abrupt loss of outer radiation belt electrons, *J. Geophys. Res.*, *112*(A01202), doi:10.1029/2006JA011708.

Roux, A., O. Le Contel, C. Coillot, A. Boubdellah, B. de la Porte, D. Alison, S. Ruocco, and M. C. Vassal (2008), The Search Coil Magnetometer for THEMIS, *Space Sci. Rev.*, submitted.

C.M. Cully, Laboratory for Atmospheric and Space Physics, University of Colorado, Boulder, CO 80303, USA. Now at Swedish Institute of Space Physics, Uppsala, Sweden. (chris.cully@irfu.se)